# Evaluating the immunoproteasome as a potential therapeutic target in cisplatin-resistant small cell and non-small cell lung cancer

Tetsuaki Shoji[1], Eiki Kikuchi[1], Junko Kikuchi[1], Yuta Takashima[1], Megumi Furuta[1], Hirofumi Takahashi[1], Kosuke Tsuji[1], Makie Maeda[1], Ichiro Kinoshita[2], Hirotoshi Dosaka-Akita[3], Jun Sakakibara-Konishi[1], Satoshi Konno[1]

[1]Department of Respiratory Medicine, Faculty of Medicine and Graduate School of Medicine, Hokkaido University, Sapporo, Hokkaido 060-8638, Japan

[2]Division of Clinical Cancer Genomics, Hokkaido University Hospital, Sapporo, Hokkaido 060-8648, Japan

[3]Department of Medical Oncology, Faculty of Medicine and Graduate School of Medicine, Hokkaido University, Sapporo, Hokkaido 060-8638, Japan

Correspondence to: Eiki Kikuchi, M.D., Ph.D.

Department of Respiratory Medicine, Faculty of Medicine and Graduate School of Medicine, Hokkaido University

N 15, W 7, Kita-Ku, Sapporo, Hokkaido 060-8638, Japan

Tel: (+81) 11-716-5911, Fax: (+81) 11-706-7899

E-mail: eikik@med.hokudai.ac.jp

**Abstract**

**Purpose:** We evaluated the expression of proteasome subunits to assess whether the proteasome could be a therapeutic target in cisplatin-resistant lung cancer cells.

**Methods:** Cisplatin-resistant (CR) variants were established from three non-small cell lung cancer (NSCLC) cell lines (A549, H1299, and H1975) and two small cell lung cancer (SCLC) cell lines (SBC3 and SBC5). The expression of proteasome subunits, the sensitivity to immunoproteasome inhibitors, and 20S proteasomal proteolytic activity were examined in the CR variants of the lung cancer cell lines.

**Results:** All five CR cell lines highly expressed one or both of the immunoproteasome subunit genes, *PSMB8* and *PSMB9*, while no clear trend was observed in the expression of constitutive proteasome subunits. The CR cells expressed significantly higher levels of PSMB8 and PSMB9 proteins as well. The CR variants of the H1299 and SBC3 cell lines were more sensitive to immunoproteasome inhibitors and had significantly more proteasomal proteolytic activity than their parental counterparts.

**Conclusions:** The immunoproteasome may be an effective therapeutic target in a subset of CR lung cancers. Proteasomal proteolytic activity may be a predictive marker for the efficacy of immunoproteasome inhibitors in cisplatin-resistant SCLC and NSCLC.

**Keywords**

Lung cancer, cisplatin resistance, immunoproteasome, immunoproteasome inhibitor, cell cycle arrest, apoptosis

## Introduction

Lung cancer is one of the most commonly diagnosed cancers and remains the most common cause of cancer-related deaths worldwide [1,2]. Lung cancer is divided into two histological classes, non-small cell lung cancer (NSCLC) (˜85% of all lung cancers) and small cell lung cancer (SCLC) (˜15%) [3]. Because recently developed molecular-targeted drugs and immune checkpoint inhibitors are effective for only a limited subset of lung cancer patients [4,5], cytotoxic chemotherapeutic agents are still widely used. Cisplatin has been used as a key drug in the treatment of patients with NSCLC and SCLC; however, the efficacy is still limited due to acquired resistance after a several months of treatment [6]. Thus, overcoming cisplatin resistance is currently an urgent issue to be addressed in NSCLC and SCLC treatment.

Cisplatin induces apoptosis by damaging DNA and inhibiting DNA synthesis [7]. Recent findings have revealed that cisplatin impairs cellular homeostasis in several ways, including oxidative stress and endoplasmic reticulum (ER) stress [8,9]. Cisplatin-induced oxidative stress inhibits calcium uptake of the mitochondria and reduces mitochondrial membrane potential, resulting in the induction of apoptosis [10]. Cisplatin-resistant (CR) cancer cells are less addicted to glycolytic pathway, and more dependent on oxidative metabolism, leading to reactive oxygen species (ROS) accumulation [11]. Cisplatin also causes the accumulation of ubiquitinated proteins and ER stress, which activate nucleus-independent apoptotic signaling [12-14].

The proteasome is a large multi-subunit complex that degrades ubiquitinated protein and reduces ER stress in eukaryotic cells [15,16]. There are two types of proteasomes, the constitutive proteasome and the immunoproteasome. The constitutive proteasome has three proteolytically active subunits, PSMB5 (also known as β5),

PSMB6 (β1), and PSMB7 (β2), which possess chymotrypsin-like, caspase-like, and trypsin-like activities, respectively. Upon exposure to inflammatory cytokines, such as IFN-γ and TNF-α, and oxidative stress, the constitutive subunits are exchanged for immunoproteasome subunits PSMB8 (β5i), PSMB9 (β1i), and PSMB10 (β2i) [17-20]. While subunits PSMB8 and PSMB10 have chymotrypsin-like and trypsin-like activities, respectively, subunit PSMB9 displays chymotrypsin-like activity rather than PSMB6-associated caspase-like activity [15]. The immunoproteasome is dominantly expressed in cells of hematologic origin and its primary function is to improve MHC class I antigen presentation [21]. The immunoproteasome has also been reported to contribute to intracellular homeostasis in concert with the constitutive proteasome [22].

Reportedly, proteasome inhibitors and immunoproteasome inhibitors (IPIs) have anti-cancer effect through ER stress-induced cell death and G2/M cell cycle arrest [23,24]. Proteasome inhibitors and IPIs have prolonged survival of patients with relapsed or refractory multiple myeloma [25-27]. In addition, several clinical trials have shown that PIs are clinically effective in a small but distinct subset of lung cancers [28-31]. Drilon et al. reported that 1 out of 16 patients with *KRAS* G12D-mutant lung adenocarcinoma, who was pretreated with carboplatin and pemetrexed and subsequent gemcitabine, showed remarkable tumor shrinkage after bortezomib treatment in a phase 2 trial [28]. Lara et al. reported that 1 out of 28 patients with platinum-refractory SCLC had a confirmed partial response after bortezomib therapy in a phase 2 trial, while none of the 28 patients with platinum-sensitive SCLC showed a clinical response [30]. Thus, platinum resistance may affect sensitivity to proteasome inhibitors in a subset of lung cancers.

Here, we examined the impact of cisplatin resistance on the expression of proteasome subunits and the cytotoxic effects of the IPIs, carfilzomib (CFZ) and PR957, in CR lung cancer cell lines. We demonstrate that two of five lung cancer cell lines obtain the sensitivity to IPI as well as acquiring cisplatin resistance and identified that the chymotrypsin-like activity of cell extract as a predictive marker for responders to IPI.

## Materials and methods

### Reagents

Cisplatin solution (Randa® Inj., 25 mg of cisplatin/50 mL of injection solution) was purchased from Nippon Kayaku, Tokyo, Japan. CFZ and PR957 (AdooQ BioScience, Irvine, CA, USA) were dissolved in dimethyl sulfoxide (DMSO) to make stock solutions of 20 mmol/L. Glutathione (GSH) and N-acetylcysteine (NAC) (Sigma-Aldrich, St. Louis, MO, USA) were dissolved in distilled water at concentrations of 50 mg/mL and 25 mg/mL, respectively.

### Cell culture and establishment of CR lung cancer cell lines

Three human NSCLC cell lines, A549, H1299, and H1975, were maintained in RPMI-1640 medium supplemented with 10% fetal bovine serum (FBS) and 100 U/mL penicillin-streptomycin in a humidified atmosphere at 37°C with 5% $CO_2$. Two human SCLC cell lines, SBC3 and SBC5, were maintained in minimum essential media supplemented with 10% FBS and 100 U/mL penicillin-streptomycin in a humidified atmosphere at 37°C with 5% $CO_2$. The CR lung cancer cell lines, A549ddpR,

H1299ddpR, H1975ddpR, SBC3ddpR, and SBC5ddpR, were established from the parental cell lines, A549, H1299, H1975, SBC3, and SBC5, respectively. The parental cells were treated with slowly increasing concentrations of cisplatin (maximum 2 μmol/L). Subsequently, they were cultured in medium containing 2 μmol/L cisplatin for 3 months.

**Cell proliferation assay**

The cytotoxic activities of cisplatin and IPIs were assessed by MTT cell proliferation assay, according to the manufacturer's instructions (Promega Corporation, Madison, WI, USA). Cells were seeded in 96-well plates at a density of $1\times10^3$–$3\times10^3$ cells per well and cultured for 24 hours prior to drug treatment. The treatment concentrations ranged from 0.001 to 50 mmol/L. 0.25% [v/v] DMSO was used as a vehicle control for IPIs, and toxicity was not observed. After treatment for 72 hours, cell viability was measured using Varioskan Flash (Thermo Fisher Scientific, Waltham, MA, USA). Half maximal inhibitory concentration (IC50) was calculated using GraphPad Prism v7.0 (GraphPad Software, San Diego, CA, USA).

**Treatment dose of CFZ**

In the analysis of cell cycle distribution, apoptosis, mitotic catastrophe, and ER stress, cells were treated with the higher of IC50 doses in the parental and the CR variant cell lines (100 nmol/L for A549 and A549ddpR, 30 nmol/L for H1299 and H1299ddpR, 40 nmol/L for SBC3 and SBC3ddpR, and 6 nmol/L for SBC5 and SBC5ddpR).

**Intracellular reactive oxygen species assay**

Intracellular ROS level was analyzed using DCFDA Cellular ROS Detection Assay Kit (Abcam, Cambridge, UK). Briefly, cells were seeded in clear bottom, dark sided 96-well microplates at a density of $1\times10^4$ cells per well. Cells were cultured overnight to adhere. Next day, cells were washed with PBS and stained with 100 μL of DCFDA (30 μmol/L) for 45 min at 37°C in the dark. After incubation, cells were washed and subjected to fluorescence measurement using Varioskan Flash (Thermo Fisher Scientific).

**Quantitative reverse transcription-PCR**

mRNA expression was determined with quantitative reverse transcription-PCR (qRT-PCR) using SYBR Green PCR Master Mix and a StepOnePlus Real-Time PCR System (Applied Biosystems, Foster City, CA, USA). Each sample was amplified in triplicate for quantification of the specified transcript level. Reactions were performed using 1 μg total RNA. *ACTB* was amplified as an internal control. mRNA levels are expressed as arbitrary units, defined as the n-fold difference relative to the control gene *ACTB* (ΔΔCt method). The primers used are listed in Supplementary Table S1.

**Western blotting and antibodies**

Whole-cell lysates were subjected to western blotting to analyze the expression of various proteins using the specific antibodies that follow. Antibodies for PSMA1 (ab3325), PSMB5 (ab3330), PSMB8 (ab3329), PSMB9 (ab3328), ubiquitinated protein (ab140601), p21 (ab109199), cyclin D (ab134175), CDK1 (phospho Y15) (ab47594), and IRE1 (phospho S724) (ab48187) were purchased from Abcam. Anti-actin antibody (#A2066) was purchased from Sigma-Aldrich (St. Louis, MO, USA). Antibodies for

cyclin A (sc-271682) and cyclin B1 (sc-166210) were purchased from Santa Cruz Biotechnology (Dallas, TX, USA). Antibodies for cleaved caspase 3 (#9661), PARP (#9532), phospho-histone H3 (Ser10) (#3377), CHOP (#2895), LC3 (#12741), and phospho-eIF2α (S51) (#9721) were purchased from Cell Signaling Technology (Danvers, MA, USA).

**20S proteasome activity assay**

The 20S proteasome chymotrypsin-like activity was analyzed using Proteasome Assay kit (Cayman Chemicals, Ann Arbor, MI, USA). Briefly, cells were seeded in 96-well cell culture plates at a density of $3\times10^4$ cells per well. Plates were centrifuged at 500 × g for 5 min and culture media was aspirated. The cells were then washed with assay buffer (Tris-buffered saline pH 8.0 with 5 mM EDTA) and lysed with 100 μL of lysis buffer. The plates were centrifuged at 1000 × g for 10 min and 90 μL of the supernatant from each well was transferred to black 96-well plates. After adding 10μL of Suc-LLVY-AMC fluorescent substrate solution, a 20S-specific chymotrypsin-like activity substrate, and incubation for 60 min at 37°C in the dark, fluorescence intensity was measured using Varioskan Flash (Thermo Fisher Scientific).

**Cell cycle and apoptosis assays**

Cell cycle and apoptosis assays were performed using a BD FACSVerse flow cytometer (Becton Dickinson, Franklin Lakes, NJ, USA). Cell cycle was analyzed using propidium iodide (PI)/RNase Staining Buffer (Becton Dickinson) and Alexa Fluor 647 Rat anti-Histone H3 (pS28) (Becton Dickinson), as per the manufacturer’s instructions. Apoptosis was analyzed using Annexin V and PI using an Annexin V-FITC Apoptosis

Detection Kit (Merck Millipore, Burlington, MA, USA), as per the manufacturer's instructions. Annexin V positive - PI negative populations represent cells in early apoptosis. Annexin V poisitive - PI positive populations indicate cells in late apoptosis [32].

**Immunofluorescence staining**

Analysis of mitotic catastrophe was performed as previously reported [33-35]. For immunofluorescence staining, cells were treated with CFZ or vehicle for 24 hours. Cells were fixed using 4% paraformaldehyde for 20 min at 4°C and permeabilized with PBS containing 0.5% Triton X-100 for 10 min at 4°C. Cells were incubated with Blocking One Histo (Nacalai Tesque, Kyoto, Japan) for 10 min at room temperature to block nonspecific antibody binding sites. Next, cells were incubated with primary antibody for β-tubulin (#2128) (Cell Signaling Technology) at 4°C overnight. They were next incubated with Alexa Flour 488 Goat anti-Rabbit IgG (Thermo Fisher Scientific) for 90 min, followed by DAPI staining. Coverslips were mounted with ProLong Diamond Antifade Mountant reagent (Thermo Fisher Scientific). Fluorescent microscopic analysis was performed using Biorevo BZ-9000 (Keyence, Osaka, Japan).

**Small interfering RNA transfection**

The CR variants of 549 and H1299 were subjected to simultaneous knockdown of PSMB5, PSMB8, and PSMB9. Small interfering RNA (siRNA) against the following genes were purchased from Horizon Discovery (Cambridge, UK): PSMB5 (E-004522-00-0005), PSMB8 (L-006022-00-0005), PSMB9 (L-006023-00-0005), and nontargeting control (D-001810-10-20). Cells were seeded in 6-well plates at a density of $2\times10^4$ cells

per well for western blot analysis and the 20S proteasome activity assay, and in 96-well plates at a density of $5\times10^3$ cells per well for MTT cell proliferation assay. Cells were transfected with 300 pmol siRNA (100 pmol of each gene) or 300 pmol nontarget control in 6-well plates and 12 pmol siRNA (4 pmol of each gene) or 12 pmol nontarget control in 96-well plates in Opti-MEM medium (Invitrogen, Waltham, MA, USA) using Lipofectamine RNAiMAX (Invitrogen). Protein for western blot analysis was collected 24, 48, and 72 hours after transfection. The 20S proteasome activity was measured 24 hours after transfection. Cells were treated with cisplatin or CFZ 24 hours after transfection for MTT cell proliferation assay.

**Statistical analysis**

All data were derived from at least three independent experiments and are shown as mean ± SD, unless otherwise indicated. Differences between groups were statistically analyzed using the Welch t test. $P<0.05$ was considered statistically significant.

## Results

### CR variants from three NSCLC and two SCLC cell lines were established

We developed the CR variants from three NSCLC cell lines (A549, H1299, and H1975) and two SCLC cell lines (SBC3 and SBC5) by treating the parental cells with an increasing concentration of cisplatin (0–2 μmol/L) over 3 months. The MTT assay showed that all five CR cell lines had a significantly decreased sensitivity to cisplatin (Fig. 1a-1e). The CR variants displayed 2.4- to 5.6-fold cisplatin resistance compared with the parental cells (Table 1). The established CR variants had higher ROS levels than their parental counterparts (Fig. 1f).

## CR variants of NSCLC and SCLC cell lines overexpress immunoproteasome subunits

First, we measured the gene expression of the 20S proteasome subunits in the parental and CR variant lung cancer cell lines using qRT-PCR. The immunoproteasome subunit *PSMB8* was highly expressed in all five CR cell lines, and *PSMB9* was also largely increased in the CR variants of all but SBC3 compared with the parental cells (Fig. 2a, Supplementary Fig. S1). On the other hand, no clear trend was observed in the expression of constitutive proteasome subunits in the CR cells. Western blot analysis revealed that the expression of the PSMB8 and PSMB9 proteins also significantly increased in the CR variants of all but SBC5 compared with the parental cells (Fig. 2b–2e). Collectively, the CR variants of the lung cancer cell lines tended to express elevated levels of the immunoproteasome subunits.

## Two of five CR variant lung cancer cell lines display increased sensitivity to immunoproteasome inhibitors

To investigate whether the CR lung cancer cell lines depend on the immunoproteasome for proliferation, we conducted an MTT cell assay using two IPIs, CFZ and PR957. Three of the five cell lines developed resistance to the IPIs when they acquired cisplatin resistance. H1299ddpR and SBC3ddpR; however, displayed significantly increased sensitivity to both CFZ and PR957 compared with their parental counterparts (Fig. 3a–e, Supplementary Fig. S2). In fact, H1299ddpR and SBC3ddpR were 2.6–15.9 fold more sensitive to the IPIs compared with their parental cell lines (Table 1). We defined cells whose sensitivity to IPIs increased while they acquired cisplatin resistance as “IPI

responders," and defined the others as "IPI non-responders." IPI responders included H1299ddpR and SBC3ddpR, and IPI non-responders included A549ddpR, H1975ddpR, and SBC5ddpR.

**IPI responders increase 20S proteasome activity more than IPI non-responders**

Next, we evaluated 20S proteasome activity using Suc-LLVY-AMC fluorescent substrate. The results revealed that all CR variants examined tended to increase chymotrypsin-like activity compared with their parental counterparts (Fig. 3f). The increase in chymotrypsin-like activity was most pronounced in the CR variant IPI responders compared with the parental cell lines. IPI responders, H1299ddpR and SBC3ddpR, displayed 2.9- to 3.5-fold more chymotrypsin-like activity compared with the H1299 and SBC3 cell lines. On the other hand, IPI non-responders displayed, at most, a 1.4-fold increase in chymotrypsin-like activity compared with the parental lines.

**Carfilzomib induces accumulation of ubiquitinated protein in IPI responders**

To investigate whether the cytotoxicity of IPIs was mediated by inhibition of proteasomal protein degradation in IPI responders, we assessed the accumulation of ubiquitinated proteins after CFZ treatment by western blot analysis. In IPI responders, CFZ-induced accumulation of ubiquitinated proteins in the CR variant cells was comparable to that of the parental cells. On the other hand, the CR variant cells of IPI non-responders reduced the ubiquitinated proteins after CFZ exposure compared to the parental cells (Supplementary fig. S3). These results suggest that CFZ displays cytotoxicity through inhibition of proteasomal protein degradation.

**Knockdown of proteasome subunits with chymotrypsin-like activity increase sensitivity to carfilzomib in IPI responder**

We reasoned that the chymotrypsin-like proteasomal activity contributes to increased sensitivity to IPIs. Therefore, we examined the effect of silencing proteasome subunits with chymotrypsin-like activity, PSMB5, PSMB8, and PSMB9 on sensitivity to CFZ or cisplatin by siRNA in the CR variants of A549 and H1299. Efficient simultaneous knockdown of PSMB5, PSMB8, and PSMB9 was confirmed through western blot analysis (Supplementary fig. S4a). Accumulation of ubiquitinated protein and suppression of 20S proteasomal chymotrypsin-like activity were also observed without impairing cell viability after the triple knockdown (Supplementary fig. 4a–c). In IPI responder H1299ddpR, the triple knockdown remarkably increased sensitivity to CFZ. On the other hand, IPI non-responder A549ddpR did not alter the CFZ sensitivity by the knockdown (Supplementary fig. S4d, Supplementary table S2). The triple knockdown also led to a small, partial restoration of the cisplatin resistance in H1299ddpR, and no apparent change was observed in A549ddpR (Supplementary fig. S4e, Supplementary table S2).

**Antioxidant agents does not affect sensitivity to carfilzomib**

We evaluated how intracellular ROS affected sensitivity to IPIs in CR cells using antioxidant agents, GSH and NAC. 1000 μmol/L of GSH or 100 μmol/L of NAC significantly reduced intracellular ROS levels in the CR cells. However, the antioxidant agents failed to show any obvious effects on sensitivity to CFZ (Supplementary fig. S5a–c).

**Carfilzomib induces apoptosis in IPI responders**

We asked whether the cytotoxic effects of IPI treatment induced apoptosis in the IPI responders. Flow cytometry analysis revealed that CFZ induced a sizable portion of IPI responder cells to apoptosis (Fig. 4a). Western blot analysis showed the accumulation of cleaved caspase-3 and cleaved PARP (Fig. 4b), confirming that CFZ induced apoptotic cell death in the IPI responders.

**Carfilzomib induces G2/M cell cycle arrest and mitotic catastrophe in IPI responders**

To clarify the characteristics of IPI-induced anti-tumor effects on IPI responders, we examined the effect of CFZ on the cell cycle by flow cytometry analysis. The CR variants of IPI responders increased or retained the CFZ-induced G2/M arrest, while IPI non-responders decreased the CFZ-induced G2/M accumulation compared to the parental cells after acquiring cisplatin resistance (Fig. 5a).

Immunofluorescent staining showed aberrant nuclei (such as micronuclei, multi-lobular nuclei, or fragmented nuclei) in the H1299ddpR cells after incubating with CFZ for 24 hours (Fig. 5b). These signs of mitotic catastrophe increased significantly in the H1299ddpR cells (IPI responders), but not in the A549ddpR cells (IPI non-responders) (Fig. 5c). Furthermore, abnormal mitosis with misaligned, dispersed chromosomes and disorganized multipolar spindles were also observed in the H1299ddpR cells after CFZ treatment (Fig. 5d). Collectively, these data suggest that CFZ (an IPI) induces G2/M cell cycle arrest and subsequent mitotic catastrophe in IPI responder cells.

To explore the molecular mechanism that triggers CFZ-induced G2/M cell cycle arrest, we examined the expression of proteins involved in controlling G2/M cell cycle progression and ER stress by western blot analysis. CFZ treatment tended to increase p21 expression in both IPI responders and non-responders. There were no proteins whose CFZ-induced changes in expression distinguished between IPI responders and IPI non-responders (Supplementary fig. S6). Accumulation of ER stress proteins such as CHOP, phospho-elF2α, and phospho-IRE1, was also observed in the cells after CFZ treatment; however, there was no difference in the expression levels of these proteins between IPI responders and IPI non-responders (Supplementary fig. S7).

**Discussion**

We developed CR cell lines from three NSCLC and two SCLC cell lines. Two of the five cell lines acquired increased sensitivity to IPI compared with their parental counterparts while developing resistance to cisplatin. This result may be consistent with the results of several clinical trials that have shown that proteasome inhibitors are clinically effective in a small but distinct subset of lung cancers, especially platinum-pretreated patients with lung cancers [28-31].

Our results show that CR lung cancer cells tend to increase the expression of the immunoproteasome subunits PSMB8 and PSMB9. The immunoproteasome can be upregulated by inflammatory cytokines, such as IFNγ, and contribute to peptide production for MHC class I antigen presentation [17]. Rouette et al. reported that upregulation of immunoproteasome expression in acute myeloid leukemia was IFN-independent and correlated with the methylation status of immunoproteasome genes. They concluded that immunoproteasome genes in human cancers were regulated by

cancer cell-extrinsic (IFN-γ) and -intrinsic (cell stress) factors [36]. The CR cell lines we established had higher ROS levels as previously reported [11]. We examined the expression of IFNγ and IFNγ receptor mRNAs in the parental and CR variant lung cancer cell lines by qRT-PCR, but IFNγ was not detected at all, and there was no significant difference in IFNγ receptor mRNA expression (data not shown). Based on these data, we hypothesize that the CR lung cancer cells increased expression of the immunoproteasome to resist cisplatin-induced cell stress, including ROS-mediated oxidative stress.

CR cell lines whose sensitivity to IPI increased while acquiring cisplatin resistance also displayed a significant increase in chymotrypsin-like activity compared with the parental cell lines. In addition, knockdown of proteasome subunits that have chymotrypsin-like activity remarkably increased sensitivity to CFZ in IPI responders. These IPI responder cells may be unduly dependent on proteasomal activity to survive while developing resistance to cisplatin. Previous studies have reported that higher immunoproteasome expression may serve as a predictive marker for proteasome and immunoproteasome inhibitor sensitivity in hematological malignancies [37,38]. IFNγ-induced upregulation of the immunoproteasome and chymotrypsin-like activity can also sensitize cancer cells to these inhibitors in hematological and solid tumors [39,40]. Our data suggest that chymotrypsin-like activity (but not upregulation of immunoproteasome proteins) may be a predictive marker for sensitivity to IPIs in CR lung cancer cells. Catalystic activity can reflect biological function more directly than protein expression and may be a more precise predictive marker for treatment response.

The simultaneous knockdown of proteasome subunits that have chymotrypsin-like activity also led to a small, partial restoration of the cisplatin

resistance in H1299ddpR. This might indicate that many factors contribute to the cisplatin resistance other than immunoproteasome dependency. We also evaluated the effect of antioxidant agents on sensitivity to CFZ and found that reduction of intracellular ROS levels by GSH or NAC did not affect the sensitivity to CFZ. The immunoproteasome dependency might be irreversible through long-term cisplatin-induced cell stress such as oxidative stress.

ER stress promotes apoptotic cell death induced by proteasome inhibitors and IPIs [16]. Cellular protein homeostasis is maintained by two major degradation pathways, the ubiquitin-proteasome system (UPS) and the autophagy-lysosome system. The autophagy-lysosome system can compensate for proteasome inhibition [41,42]. Our data show that the expression of ER stress proteins was elevated after CFZ treatment in both IPI responders and non-responders. IPI non-responders may rely on UPS-independent proteolysis.

CFZ induced G2/M cell cycle arrest and subsequent mitotic catastrophe in the IPI responder cells. Prior studies found that upregulation of p21 is involved in G2/M cell cycle arrest induced by proteasomal inhibitors and IPIs [43,44], and p21 is a negative regulator of G1/S cell cycle progression [45]; however, we found that p21 expression was elevated in both IPI responders and non-responders. These data suggest that p21 may not be the factor responsible for IPI-induced cytotoxicity in the CR lung cancer cell lines. We could not identify an element that might explain the effect of IPIs in the IPI responder cells. However, we would presume that factors involved in G2/M cell cycle progression might be the target of IPIs.

In conclusion, the immunoproteasome may be a therapeutic target in a subset of CR lung cancers, and proteasomal proteolytic activity may be a predictive marker for

the efficacy of IPIs in CR lung cancer. Our preclinical results suggest IPIs as potential treatment alternatives for cisplatin-resistant SCLC and NSCLC.

## Compliance with ethical standards

## Conflict of interest

The authors declare that they have no conflict of interest.

## Ethical approval

This article does not contain any studies with human participants or animals performed by any of the authors.

## Prior presentation

This article has been presented in part at World Conference on Lung Cancer 2019, Barcelona, Spain, September 7–10, 2019. The abstract appeared in Journal of Thoracic Oncology, Volume 14, Issue 10, Supplement, October 2019, Page S705.

## References

1. Torre LA, Bray F, Siegel RL, Ferlay J, Lortet-Tieulent J, Jemal A (2015) Global cancer statistics, 2012. CA Cancer J Clin 65 (2):87-108. https://doi.org/10.3322/caac.21262

2. Siegel RL, Miller KD, Jemal A (2019) Cancer statistics, 2019. CA Cancer J Clin 69 (1):7-34. https://doi.org/10.3322/caac.21551

3. Herbst RS, Heymach JV, Lippman SM (2008) Lung cancer. N Engl J Med 359 (13):1367-1380. https://doi.org/10.1056/NEJMra0802714

4. Hirsch FR, Scagliotti GV, Mulshine JL, Kwon R, Curran WJ, Wu Y-L, Paz-Ares L (2017) Lung cancer: current therapies and new targeted treatments. Lancet 389 (10066):299-311. https://doi.org/10.1016/s0140-6736(16)30958-8

5. Tay RY, Heigener D, Reck M, Califano R (2019) Immune checkpoint blockade in small cell lung cancer. Lung Cancer 137:31-37. https://doi.org/10.1016/j.lungcan.2019.08.024

6. Amable L (2016) Cisplatin resistance and opportunities for precision medicine. Pharmacol Res 106:27-36. https://doi.org/10.1016/j.phrs.2016.01.001

7. Basu A, Krishnamurthy S (2010) Cellular responses to cisplatin-induced DNA damage. J Nucleic Acids. https://doi.org/10.4061/2010/201367

8. Brozovic A, Ambriović-Ristov A, Osmak M (2010) The relationship between cisplatin-induced reactive oxygen species, glutathione, and BCL-2 and resistance to cisplatin. Crit Rev Toxicol 40 (4):347-359. https://doi.org/10.3109/10408441003601836

9. Mandic A, Hansson J, Linder S, Shoshan MC (2003) Cisplatin induces endoplasmic reticulum stress and nucleus-independent apoptotic signaling. J Biol Chem 278 (11):9100-9106. https://doi.org/10.1074/jbc.M210284200

10. Cocetta V, Ragazzi E, Montopoli M (2019) Mitochondrial involvement in cisplatin resistance. Int J Mol Sci 20 (14). https://doi.org/10.3390/ijms20143384

11. Wangpaichitr M, Sullivan EJ, Theodoropoulos G, Wu C, You M, Feun LG, Lampidis TJ, Kuo MT, Savaraj N (2012) The relationship of thioredoxin-1 and cisplatin resistance: its impact on ROS and oxidative metabolism in lung cancer cells. Mol Cancer Ther 11 (3):604-615. https://doi:10.1158/1535-7163.MCT-11-0599

12. Xu Y, Yu H, Qin H, Kang J, Yu C, Zhong J, Su J, Li H, Sun L (2012) Inhibition of autophagy enhances cisplatin cytotoxicity through endoplasmic reticulum stress in human cervical cancer cells. Cancer Lett 314 (2):232-243. https://doi.org/10.1016/j.canlet.2011.09.034

13. Martins I, Kepp O, Schlemmer F, Adjemian S, Tailler M, Shen S, Michaud M,

455 Menger L, Gdoura A, Tajeddine N, Tesniere A, Zitvogel L, Kroemer G (2011)
456 Restoration of the immunogenicity of cisplatin-induced cancer cell death by
457 endoplasmic reticulum stress. Oncogene 30 (10):1147-1158.
458 https://doi.org/10.1038/onc.2010.500
459 14. Xu Y, Wang C, Li Z (2014) A new strategy of promoting cisplatin chemotherapeutic
460 efficiency by targeting endoplasmic reticulum stress. Mol Clin Oncol 2 (1):3-7.
461 https://doi.org/10.3892/mco.2013.202
462 15. Murata S, Takahama Y, Kasahara M, Tanaka K (2018) The immunoproteasome and
463 thymoproteasome: functions, evolution and human disease. Nat Immunol 19 (9):923-
464 931. https://doi.org/10.1038/s41590-018-0186-z
465 16. Nikesitch N, Lee JM, Ling S, Roberts TL (2018) Endoplasmic reticulum stress in
466 the development of multiple myeloma and drug resistance. Clin Transl Immunology
467 7 (1):e1007. https://doi.org/10.1002/cti2.1007
468 17. Aki M, Shimbara N, Takashina M, Akiyama K, Kagawa S, Tamura T, Tanahashi N,
469 Yoshimura T, Tanaka K, Ichihara A (1994) Interferon-gamma induces different
470 subunit organizations and functional diversity of proteasomes. J Biochem 115
471 (2):257-269. https://doi.org/10.1093/oxfordjournals.jbchem.a124327
472 18. Hallermalm K, Seki K, Wei C, Castelli C, Rivoltini L, Kiessling R, Levitskaya J

(2001) Tumor necrosis factor-alpha induces coordinated changes in major histocompatibility class I presentation pathway, resulting in increased stability of class I complexes at the cell surface. Blood 98 (4):1108-1115

19. Thomas S, Kotamraju S, Zielonka J, Harder DR, Kalyanaraman B (2007) Hydrogen peroxide induces nitric oxide and proteosome activity in endothelial cells: a bell-shaped signaling response. Free Radic Biol Med 42 (7):1049-1061. https://doi.org/10.1016/j.freeradbiomed.2007.01.005

20. Pickering AM, Koop AL, Teoh CY, Ermak G, Grune T, Davies KJ (2010) The immunoproteasome, the 20S proteasome and the PA28alphabeta proteasome regulator are oxidative-stress-adaptive proteolytic complexes. Biochem J 432 (3):585-594. https://doi.org/10.1042/BJ20100878

21. Groettrup M, Kirk CJ, Basler M (2010) Proteasomes in immune cells: more than peptide producers? Nat Rev Immunol 10 (1):73-78. https://doi.org/10.1038/nri2687

22. Nathan JA, Spinnenhirn V, Schmidtke G, Basler M, Groettrup M, Goldberg AL (2013) Immuno- and constitutive proteasomes do not differ in their abilities to degrade ubiquitinated proteins. Cell 152 (5):1184-1194. https://doi.org/10.1016/j.cell.2013.01.037

23. Gandolfi S, Laubach JP, Hideshima T, Chauhan D, Anderson KC, Richardson PG

(2017) The proteasome and proteasome inhibitors in multiple myeloma. Cancer Metastasis Rev 36 (4):561-584. https://doi.org/10.1007/s10555-017-9707-8

24. Roeten MSF, Cloos J, Jansen G (2018) Positioning of proteasome inhibitors in therapy of solid malignancies. Cancer Chemother Pharmacol 81 (2):227-243. https://doi.org/10.1007/s00280-017-3489-0

25. Richardson PG, Sonneveld P, Schuster MW, Irwin D, Stadtmauer EA, Facon T, Harousseau JL, Ben-Yehuda D, Lonial S, Goldschmidt H, Reece D, San-Miguel JF, Bladé J, Boccadoro M, Cavenagh J, Dalton WS, Boral AL, Esseltine DL, Porter JB, Schenkein D, Anderson KC; Assessment of Proteasome Inhibition for Extending Remission (APEX) Investigators (2005) Bortezomib or high-dose dexamethasone for relapsed multiple myeloma. N Engl J Med 352 (24):2487-2498. https://doi.org/10.1056/NEJMoa043445

26. Dimopoulos MA, Goldschmidt H, Niesvizky R, Joshua D, Chng W-J, Oriol A, Orlowski RZ, Ludwig H, Facon T, Hajek R, Weisel K, Hungria V, Minuk L, Feng S, Zahlten-Kumeli A, Kimball AS, Moreau P (2017) Carfilzomib or bortezomib in relapsed or refractory multiple myeloma (ENDEAVOR): an interim overall survival analysis of an open-label, randomised, phase 3 trial. Lancet Oncol 18 (10):1327-1337. https://doi.org/10.1016/s1470-2045(17)30578-8

27. Moreau P, Masszi T, Grzasko N, Bahlis NJ, Hansson M, Pour L, Sandhu I, Ganly P, Baker BW, Jackson SR, Stoppa AM, Simpson DR, Gimsing P, Palumbo A, Garderet L, Cavo M, Kumar S, Touzeau C, Buadi FK, Laubach JP, Berg DT, Lin J, Di Bacco A, Hui AM, van de Velde H, Richardson PG, Group T-MS (2016) Oral Ixazomib, Lenalidomide, and Dexamethasone for Multiple Myeloma. N Engl J Med 374 (17):1621-1634. https://doi.org/10.1056/NEJMoa1516282

28. Drilon A, Schoenfeld AJ, Arbour KC, Litvak A, Ni A, Montecalvo J, Yu HA, Panora E, Ahn L, Kennedy M, Haughney-Siller A, Miller V, Ginsberg M, Ladanyi M, Arcila M, Rekhtman N, Kris MG, Riely GJ (2019) Exceptional responders with invasive mucinous adenocarcinomas: a phase 2 trial of bortezomib in patients with KRAS G12D-mutant lung cancers. Cold Spring Harb Mol Case Stud 5 (2). https://doi.org/10.1101/mcs.a003665

29. Papadopoulos KP, Burris HA 3rd, Gordon M, Lee P, Sausville EA, Rosen PJ, Patnaik A, Cutler RE, Jr., Wang Z, Lee S, Jones SF, Infante JR (2013) A phase I/II study of carfilzomib 2-10-min infusion in patients with advanced solid tumors. Cancer Chemother Pharmacol 72 (4):861-868. https://doi.org/10.1007/s00280-013-2267-x

30. Lara PN Jr, Chansky K, Davies AM, Franklin WA, Gumerlock PH, Gualianone PP,

Atkins JN, Farneth N, Mack PC, Crowley JJ, Gandara DR (2006) Bortezomib (PS-341) in relapsed or refractory extensive stage small cell lung cancer: a Southwest Oncology Group phase II trial (S0327). J Thorac Oncol 1 (9):996-1001

31. Arnold SM, Chansky K, Leggas M, Thompson MA, Villano JL, Hamm J, Sanborn RE, Weiss GJ, Chatta G, Baggstrom MQ (2017) Phase 1b trial of proteasome inhibitor carfilzomib with irinotecan in lung cancer and other irinotecan-sensitive malignancies that have progressed on prior therapy (Onyx IST reference number: CAR-IST-553). Invest New Drugs 35 (5):608-615. https://doi.org/10.1007/s10637-017-0441-4

32. Vermes I, Haanen C, Reutelingsperger C (2000) Flow cytometry of apoptotic cell death. J Immunol Methods 243 (1-2):167-190. https://doi:10.1016/s0022-1759(00)00233-7

33. Suzuki M, Yamamori T, Yasui H, Inanami O (2016) Effect of MPS1 Inhibition on Genotoxic Stress Responses in Murine Tumour Cells. Anticancer Res 36 (6):2783-2792

34. Suzuki M, Yamamori T, Bo T, Sakai Y, Inanami O (2017) MK-8776, a novel Chk1 inhibitor, exhibits an improved radiosensitizing effect compared to UCN-01 by exacerbating radiation-induced aberrant mitosis. Transl Oncol 10 (4):491-500.

https://doi.org/10.1016/j.tranon.2017.04.002

35. Takashima Y, Kikuchi E, Kikuchi J, Suzuki M, Kikuchi H, Maeda M, Shoji T, Furuta M, Kinoshita I, Dosaka-Akita H, Sakakibara-Konishi J, Konno S (2019) Bromodomain and extraterminal domain inhibition synergizes with WEE1-inhibitor AZD1775 effect by impairing nonhomologous end joining and enhancing DNA damage in nonsmall cell lung cancer. Int J Cancer. https://doi.org/10.1002/ijc.32515

36. Rouette A, Trofimov A, Haberl D, Boucher G, Lavallee VP, D'Angelo G, Hebert J, Sauvageau G, Lemieux S, Perreault C (2016) Expression of immunoproteasome genes is regulated by cell-intrinsic and -extrinsic factors in human cancers. Sci Rep 6:34019. https://doi.org/10.1038/srep34019

37. Niewerth D, Franke NE, Jansen G, Assaraf YG, van Meerloo J, Kirk CJ, Degenhardt J, Anderl J, Schimmer AD, Zweegman S, de Haas V, Horton TM, Kaspers GJ, Cloos J (2013) Higher ratio immune versus constitutive proteasome level as novel indicator of sensitivity of pediatric acute leukemia cells to proteasome inhibitors. Haematologica 98 (12):1896-1904. https://doi.org/10.3324/haematol.2013.092411

38. Niewerth D, Kaspers GJ, Jansen G, van Meerloo J, Zweegman S, Jenkins G, Whitlock JA, Hunger SP, Lu X, Alonzo TA, van de Ven PM, Horton TM, Cloos J (2016) Proteasome subunit expression analysis and chemosensitivity in relapsed

563 paediatric acute leukaemia patients receiving bortezomib-containing chemotherapy. J
564 Hematol Oncol 9 (1):82. https://doi.org/10.1186/s13045-016-0312-z
565 39. Niewerth D, Kaspers GJ, Jansen G, van Meerloo J, Zweegman S, Jenkins G,
566 Whitlock JA, Hunger SP, Lu X, Alonzo TA, van de Ven PM, Horton TM, Cloos J
567 (2014) Interferon-γ-induced upregulation of immunoproteasome subunit assembly
568 overcomes bortezomib resistance in human hematological cell lines. J Hematol
569 Oncol 7 (7). https://doi.org/10.1186/1756-8722-7-7
570 40. Busse A, Kraus M, Na IK, Rietz A, Scheibenbogen C, Driessen C, Blau IW, Thiel E,
571 Keilholz U (2008) Sensitivity of tumor cells to proteasome inhibitors is associated
572 with expression levels and composition of proteasome subunits. Cancer 112 (3):659-
573 670. https://doi.org/10.1002/cncr.23224
574 41. Ji CH, Kwon YT (2017) Crosstalk and Interplay between the Ubiquitin-Proteasome
575 System and Autophagy. Mol Cells 40 (7):441-449.
576 https://doi.org/10.14348/molcells.2017.0115
577 42. Zaffagnini G, Martens S (2016) Mechanisms of Selective Autophagy. J Mol Biol
578 428 (9 Pt A):1714-1724. https://doi.org/10.1016/j.jmb.2016.02.004
579 43. Ling YH, Liebes L, Jiang JD, Holland JF, Elliott PJ, Adams J, Muggia FM, Perez-
580 Soler R (2003) Mechanisms of proteasome inhibitor PS-341-induced G(2)-M-phase

581 arrest and apoptosis in human non-small cell lung cancer cell lines. Clin Cancer Res
582 9 (3):1145-1154
583 44. Zang L, Boufraqech M, Lake R, Kebebew E (2016) Carfilzomib potentiates CUDC-
584 101-induced apoptosis in anaplastic thyroid cancer. Oncotarget 7 (13):16517-16528.
585 https://doi.org/10.18632/oncotarget.7760
586 45. Sherr CJ, Roberts JM (1999) CDK inhibitors: positive and negative regulators of
587 G1-phase progression. Genes Dev 13 (12):1501-1512.
588 https://doi.org/10.1101/gad.13.12.1501
589

590 **Table 1** IC50 values of cisplatin, carfilzomib, and PR957. Data represent the mean ±
591 SD of 3 independent experiments. IC50, half maximal inhibitory concentration; CR,
592 cisplatin-resistant.

| | IC50 values of cisplatin (μmol/L) | | | IC50 values of carfilzomib (nmol/L) | | | IC50 values of PR957 (μmol/L) | | |
|---|---|---|---|---|---|---|---|---|---|
| | Parental | CR variant | *P* | Parental | CR variant | *P* | Parental | CR variant | *P* |
| A549 | 3.8±0.2 | 14.1±2.1 | <0.05 | 12.9±5.9 | 97.5±42.0 | <0.05 | 0.91±0.11 | 7.03±4.22 | 0.13 |
| H1299 | 3.6±2.2 | 8.8±2.2 | <0.05 | 28.9±1.6 | 3.2±1.2 | <0.01 | 1.48±0.17 | 0.26±0.07 | <0.01 |
| H1975 | 3.1±0.1 | 9.3±0.4 | <0.01 | 2.4±1.9 | 33.8±20.4 | 0.12 | 0.14±0.06 | 0.84±0.44 | 0.11 |
| SBC3 | 1.3±0.4 | 7.0±0.4 | <0.01 | 42.8±2.0 | 16.3±6.1 | <0.05 | 12.7±6.1 | 0.80±0.28 | <0.05 |
| SBC5 | 2.7±0.8 | 15.0±2.0 | <0.01 | 3.9±0.5 | 5.7±0.8 | 0.08 | 0.40±0.04 | 0.41±0.08 | 0.88 |

593

594

595 **Figure legends**

596 **Fig. 1** Cisplatin-resistant (CR) lung cancer cell lines are less sensitive to cisplatin (**a**)
597 A549 and the CR variant, A549ddpR (**b**) H1299 and the CR variant, H1299ddpR (**c**)
598 H1975 and the CR variant, H1975ddpR (**d**) SBC3 and the CR variant, SBC3ddpR (**e**)
599 SBC5 and the CR variant, SBC5ddpR. All cell lines were treated with cisplatin for 72
600 hours, then proliferation was assessed with an MTT assay. (**f**) Intracellular reactive
601 oxygen species (ROS) levels were analyzed in the parental and CR variant lung cancer
602 cell lines using DCFDA. **P*<0.05, ***P*<0.01, ****P*<0.001, Welch t test.
603
604 **Fig. 2** Immunoproteasome subunits tend to be highly expressed in cisplatin-resistant
605 (CR) cell lines (**a**) Relative expression of constitutive and immunoproteasome subunits
606 determined by quantitative reverse transcription PCR (qRT-PCR) analysis of the CR
607 variant cell lines derived from A549, H1299, H1975, SBC3, and SBC5, and normalized
608 to expression in their parental counterparts. (**b, c**) Western blot analysis showing that
609 PSMB8 and PSMB9 tend to be highly expressed in the CR variants derived from (**b**)
610 three non-small cell lung cancer cell lines and (**c**) two small cell lung cancer cell lines.
611 (**d**) Quantification of western blot analysis shown in (**b**) and normalized to actin. (**e**)
612 Quantification of western blot analysis shown in (**c**) and normalized to actin. **P*<0.05,
613 ***P*<0.01, ****P*<0.001, Welch t test.
614
615 **Fig. 3** The effect of the immunoproteasome inhibitor (IPI), carfilzomib, on cisplatin-
616 resistant (CR) variants derived from (**a**) A549, (**b**) H1299, (**c**) H1975, (**d**) SBC3, and (**e**)
617 SBC5 lung cancer cell lines by MTT assay. (**f**) 20S proteasome chymotrypsin-like
618 activity was analyzed in CR lung cancer cell line variants and their parental cell lines.

20S proteasome activity increased more in IPI responder variants than IPI non-responder variants. *$P$<0.05, **$P$<0.01, Welch t test.

**Fig. 4** (**a**) CFZ-induced apoptosis is elevated in IPI responder cell lines. Apoptotic cells were analyzed using flow cytometry and Annexin V/propidium iodide (PI) staining. (**b**) Western blots showing that CFZ treatment resulted in elevated levels of cleaved caspase-3 and cleaved PARP in IPI responder cell lines.

**Fig. 5** (**a**) The cisplatin-resistant (CR) variants of IPI responders increased or retained the CFZ (carfilzomib)-induced G2/M arrest, while IPI non-responders decreased the CFZ-induced G2/M accumulation compared to the parental cells after acquiring cisplatin resistance. Cell cycle phase distributions were determined by flow cytometry with propidium iodide (PI) and anti-phospho-histone H3 antibody. (**b**) Representative images of CR variants from H1299 cells possessing features of mitotic catastrophe, such as micronuclei, fragmented nuclei, and multi-lobular nuclei. (**c**) Bar chart showing percentages of CR variants from A549 and H1299 cells undergoing mitotic catastrophe. (**d**) Representative images of abnormal mitoses in CR variants derived from H1299 cells after treatment with CFZ. Scale bars represent 10 μm. **$P$<0.01, Welch t test.

Figure 1.

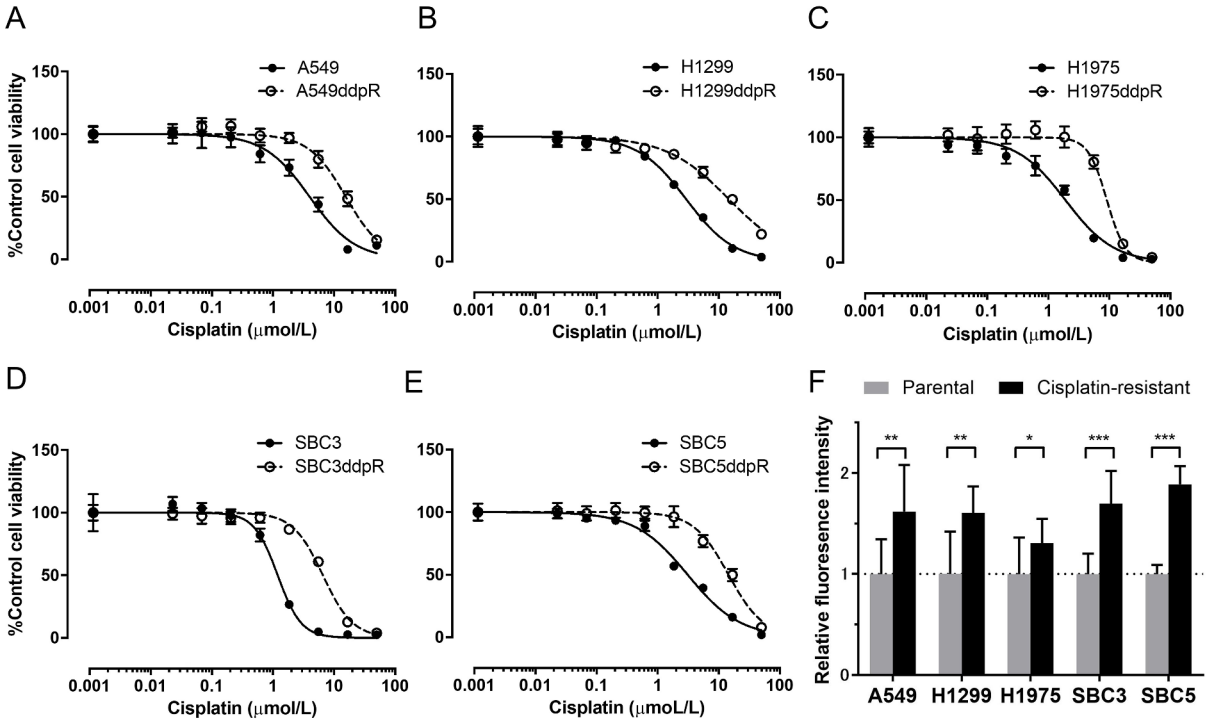
A
B
C
D
E
F
A549
A549ddpR
H1299
H1299ddpR
H1975
H1975ddpR
SBC3
SBC3ddpR
SBC5
SBC5ddpR
%Control cell viability
Cisplatin (μmol/L)
Cisplatin (μmoL/L)
Parental
Cisplatin-resistant
Relative fluoresence intensity
A549
H1299
H1975
SBC3
SBC5

Figure 2.

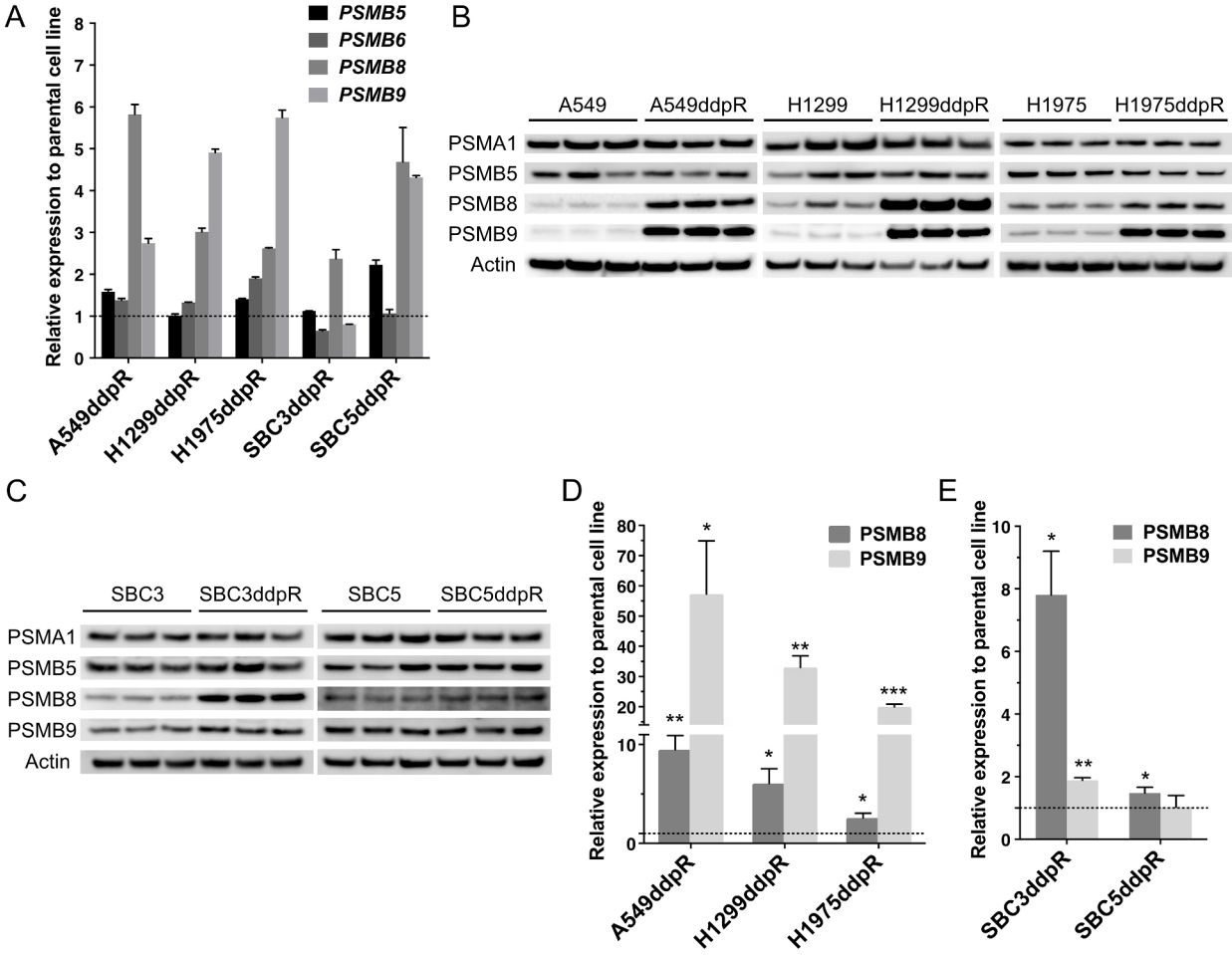
A
Relative expression to parental cell line
PSMB5
PSMB6
PSMB8
PSMB9
A549ddpR
H1299ddpR
H1975ddpR
SBC3ddpR
SBC5ddpR
B
A549
A549ddpR
H1299
H1299ddpR
H1975
H1975ddpR
PSMA1
PSMB5
PSMB8
PSMB9
Actin
C
SBC3
SBC3ddpR
SBC5
SBC5ddpR
PSMA1
PSMB5
PSMB8
PSMB9
Actin
D
Relative expression to parental cell line
PSMB8
PSMB9
A549ddpR
H1299ddpR
H1975ddpR
E
Relative expression to parental cell line
PSMB8
PSMB9
SBC3ddpR
SBC5ddpR

Figure 3.

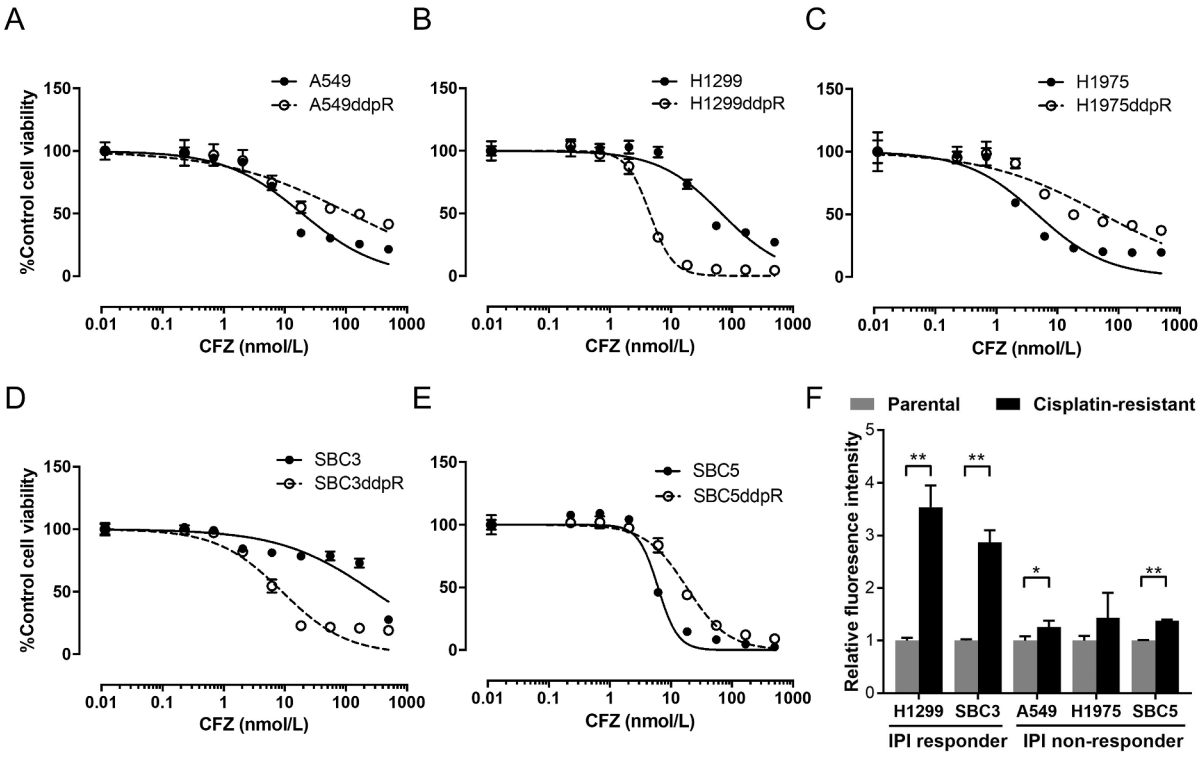
A
B
C
D
E
F
A549
A549ddpR
H1299
H1299ddpR
H1975
H1975ddpR
SBC3
SBC3ddpR
SBC5
SBC5ddpR
%Control cell viability
CFZ (nmol/L)
Parental
Cisplatin-resistant
Relative fluoresence intensity
H1299
SBC3
A549
H1975
SBC5
IPI responder
IPI non-responder

Figure 4.

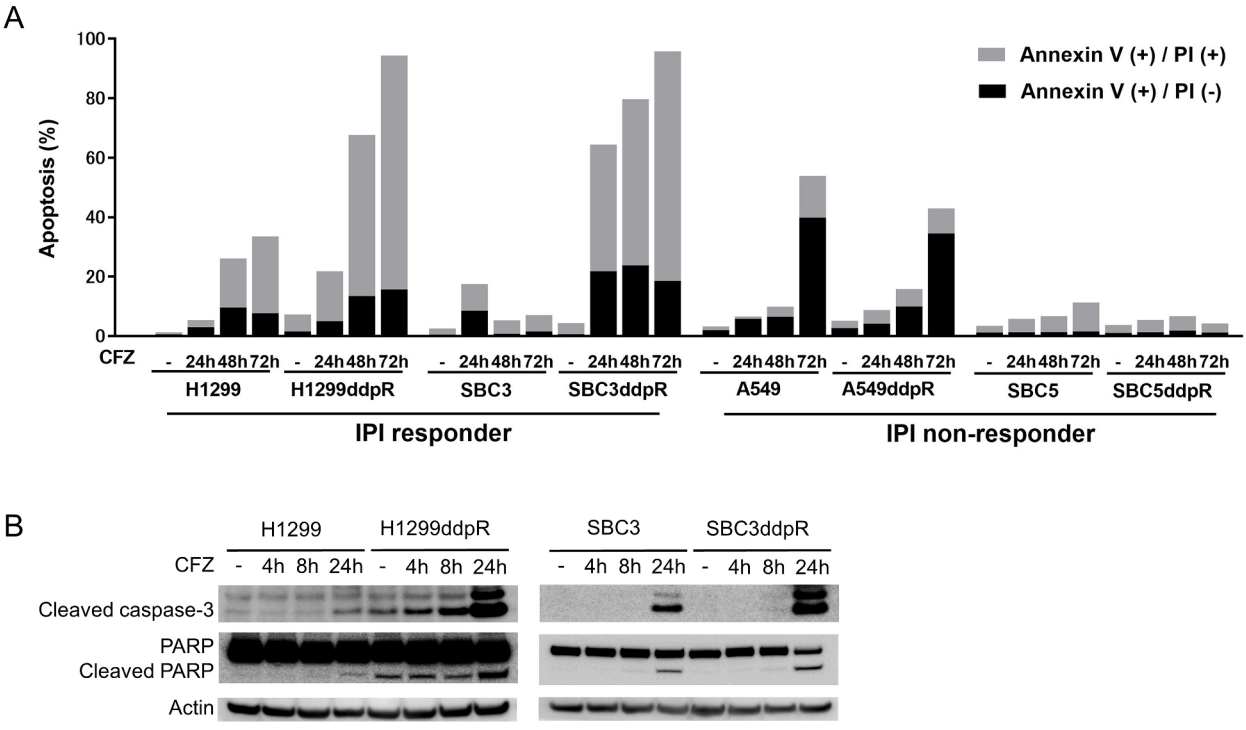
A
Annexin V (+) / PI (+)
Annexin V (+) / PI (-)
Apoptosis (%)
100
80
60
40
20
0
CFZ
- 24h 48h 72h
H1299
H1299ddpR
SBC3
SBC3ddpR
A549
A549ddpR
SBC5
SBC5ddpR
IPI responder
IPI non-responder
B
H1299
H1299ddpR
SBC3
SBC3ddpR
CFZ - 4h 8h 24h
Cleaved caspase-3
PARP
Cleaved PARP
Actin

Figure 5.

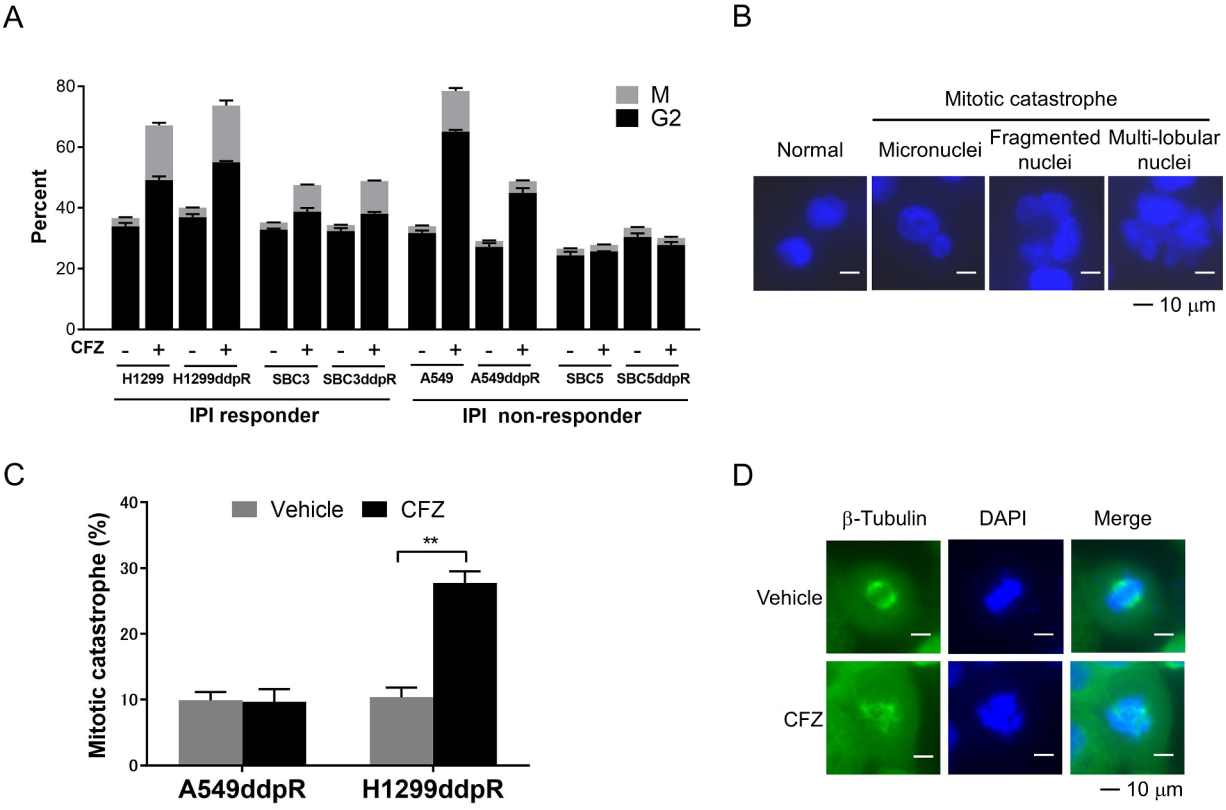
A
80
60
40
20
0
Percent
M
G2
CFZ
- + - + - + - + - + - + - + - +
H1299
H1299ddpR
SBC3
SBC3ddpR
A549
A549ddpR
SBC5
SBC5ddpR
IPI responder
IPI non-responder
B
Mitotic catastrophe
Normal
Micronuclei
Fragmented nuclei
Multi-lobular nuclei
10 μm
C
Vehicle
CFZ
**
Mitotic catastrophe (%)
40
30
20
10
0
A549ddpR
H1299ddpR
D
β-Tubulin
DAPI
Merge
Vehicle
CFZ
10 μm